Conjugation of Peptides to the Passivation Shell of Gold Nanoparticles for Targeting of Cell-Surface Receptors

Lisa Maus,[†] Oliver Dick,[‡] Hilmar Bading,[‡] Joachim P. Spatz,[†] and Roberto Fiammengo[†,*]

[†]Department of New Materials and Biosystems, Max Planck Institute for Metals Research, Stuttgart, Germany, and Department of Biophysical Chemistry, University of Heidelberg, Germany, postal address: Heisenbergstrasse 3, 70569 Stuttgart, Germany, and [‡]Department of Neurobiology, Interdisciplinary Center for Neurosciences (IZN), University of Heidelberg, Im Neuenheimer Feld 364, 69120 Heidelberg, Germany

ABSTRACT We report the preparation of gold nanoparticles (AuNPs) functionalized with the peptide-toxin conantokin-G and their selective binding to *N*-methyl-D-aspartate (NMDA) receptors recombinantly expressed by transfected HEK 293 cells. The AuNPs are passivated with a mixed self-assembled monolayer of ω-carboxy- and ω-amino-polyethylene glycol (PEG) thiols. We compare two different passivation systems: the alkyl-PEG600 system is characterized by a C_{11}-alkyl chain between the thiol group and the PEG segment, whereas the PEG3000 system lacks this alkyl-chain. We show that only the alkyl-PEG600 passivation system allows selective conjugation of cysteine-terminated peptides to the periphery of the passivation layer *via* a heterobifunctional linker strategy. In contrast, using the PEG3000 passivation system, peptides are immobilized both on the passivation layer and directly on the gold surface *via* concurrent place-exchange reaction. We therefore recommend the use of the alkyl-PEG600 system to precisely control the number of immobilized peptides on AuNPs. In fact, we show that the number of conjugated peptides per particle can be varied with good control simply by varying the composition of the self-assembled monolayer. Finally, we demonstrate that conjugation of the conantokin-G peptide to the solvent-exposed interface of the passivation layer results in maximal binding interaction between the peptide-functionalized AuNPs and the targeted NMDA receptors on the cell surface. Conantokin G-coupled AuNP may be used to spatially restrict NMDA-receptor-blockade on neuronal surfaces.

KEYWORDS: gold nanoparticles · PEG · peptides · conantokin G · NMDA receptors · multivalency

Functionalized nanoparticles which specifically interact with cellular targets are of great interest in biotechnology and biomedicine and for the development of biodiagnostics.[1−3] Gold nanoparticles (AuNPs) in particular have been established as versatile tools for various biotechnological applications.[4−8] For example, AuNPs have been functionalized with cell penetrating peptides to improve internalization[9−12] or with RME, NLS, and Tat peptides to target the cell nucleus,[11,13−16] showing that functionalization with peptides is a powerful strategy for achieving selectivity and versatility.

The most straightforward way to prepare peptide-functionalized AuNPs is by direct immobilization of thiol terminated peptides on the gold surface of the nanoparticle. In this case, the immobilized peptides also serve as stabilizers of the colloidal solution by forming a passivation layer, thus preventing aggregation of the AuNPs. However, it has been recognized that only in some cases, that is, for certain amino acid sequences,[17,18] can a sufficient stabilization of the colloidal solution be achieved using peptides as stabilizers. An alternative and valuable approach for the preparation of peptide-functionalized AuNPs requires a deliberate separation of the functionalization process from the passivation process. Bioactive peptides have been covalently conjugated to proteins such as BSA[10,15,19] and streptavidin,[20] and the conjugates have been used for stabilization/functionalization of AuNPs. These modified proteins adsorb on the gold surface of the nanoparticles, forming a passivation layer and, at the same time, serve as loading platforms for the bioactive peptides. Excellent results have also been achieved by preparing mixed monolayers of peptides[21,22] or of poly(ethylene glycol) (PEG) derivatives and peptides.[11,23,24] In these cases, one component of the mixed monolayer is present in excess and determines the stability of the colloidal solution toward aggregation while the other serves as the bioactive component. Alternatively, AuNPs can be stabilized with a passivation layer before coupling of the bioactive peptides to the passivation layer itself *via* suitable linkers.[25] Recently, we have proposed a variant of this approach where a bioactive peptide is coupled to AuNPs passivated with mixed-monolayers of ω-functionalized PEG-thiols.[26] In our system, ω-carboxyl PEG-thiols are responsible for colloidal stabilization while a small amount of ω-amino PEG-thiol

*Address correspondence to fiammengo@mf.mpg.de

Received for review August 2, 2010 and accepted October 07, 2010.

Published online October 12, 2010. 10.1021/nn101867w

derivatives is introduced for covalent functionalization.

Methods allowing immobilization of the peptides onto the solvent-exposed interface of the passivation layer are expected to maximize the accessibility of the peptides, affording AuNPs with improved performance for biotechnological application. However, this hypothesis has not yet been tested due to the lack of an appropriate model system. In this work, we describe the preparation and characterization of such a system. In fact, we show for the first time that bioactive peptides can be selectively coupled either on the passivation layer or within the passivation layer, depending on the choice of the PEG-thiol derivatives used for nanoparticle passivation. We compare AuNPs passivated with alkyl-PEG600 thiols (**1** and **2**) *versus* AuNPs passivated with PEG3000 thiols (**3** and **4**) with respect to stability, peptide coupling, and performance when targeting cell-surface receptors. We have discovered that it is possible to conjugate cysteine-terminated peptides selectively to the passivation layer of AuNPs *via* a linker strategy if the nanoparticles are passivated with alkyl-PEG600 thiols. In contrast, for PEG3000 passivated AuNPs, cysteine-terminated peptides are also immobilized in the absence of the linker, most probably in a place-exchange reaction.[27] AuNPs carrying the bioactive peptide conantokin-G (ConG) immobilized onto the solvent-exposed interface of the passivation layer (alkyl-PEG600 thiols **1**/**2**) are shown to have an improved binding performance when targeting *N*-methyl-D-aspartate (NMDA) receptors compared to AuNPs with ConG immobilized within the passivation layer (PEG3000 thiols **3**/**4**).

For both passivation systems, multiple copies of a peptide are immobilized on the AuNPs. The multivalent nature[28] of these objects is expected to be advantageous for increasing the binding affinity[29−31] and can be of great relevance if the interaction between peptide ligand (conjugated to the AuNP) and cellular receptor is not very strong. Furthermore, it would be highly desirable to have a strategy for controlling the multivalent nature of AuNP−peptide conjugates. Here we show that the number of coupled peptides, can be simply controlled by varying the number of functionalizable groups introduced in the passivation layer. However, this is true only for the passivation system based on alkyl-PEG600 thiols **1**/**2**. In contrast, control over the number of coupled peptides is not achievable for the passivation system based on PEG3000 thiols **3**/**4** due to concomitant place-exchange reaction. As a direct consequence of the AuNPs multivalency, the binding constant for immobilized ConG to the NMDA receptors is approximately 3 orders of magnitude higher than for free ConG in solution.

RESULTS AND DISCUSSION

Preparation of AuNPs with a Predetermined Diameter. One of the most used methods for the preparation of uniform AuNPs with controlled size above 10 nm is the direct reduction of gold ions by citrate.[32−34] Although this method allows reproducible preparation of spherical nanoparticles with diameters in the range 10−20 nm, nanoparticles larger than 30 nm tend to have a rather elliptical shape and relatively high dispersity (size distributions with 15−20% relative standard deviation).[35] Alternatively, the seeded-growth method generally provides better control of dimension and shape of the nanoparticles.[36] For this method, a growth solution containing $AuCl_4^-$ ions and a mild reducing agent is inoculated with a certain amount of small particles (seeds). Under these conditions, the gold ions are selectively reduced at the nanoparticle surface (nanoparticle growth), while new particle nucleation is prevented.[32,35] Several reducing agents, such as citrate,[35] ascorbate,[36,37] acrylate,[38] 2-mercaptosuccinic acid,[39] and hydroxylamine hydrochloride,[35,40] have been proposed, sometimes in combination with surfactants such as CTAB to further improve the control over the shape of the nanoparticles.[36,37]

We have developed a novel, simple, and reproducible experimental protocol for the preparation of nearly spherical gold nanoparticles based on a single-step seeded-growth reaction. The key step of our growth protocol is the controlled addition of a 6.5×10^{-4} M $HAuCl_4$ aqueous solution to an aqueous hydroxylamine hydrochloride solution containing nanoparticle seeds at a concentration between 3.5 and 7.7×10^{11} particle/mL. In practice, seed particles are prepared by the standard citrate synthesis using the experimental conditions reported by Grabar.[41] The AuNP-seed solution is mixed with a 10 mM $NH_2OH \cdot HCl$ solution in a 1:12 ratio by volume. The gold chloride solution is then added at a constant flow of 50 mL/h under vigorous stirring at room temperature. A standard growth reaction can be carried out within one to a few hours, depending on the amount of starting particles and their desired final size. Under these conditions, we consistently obtain AuNPs having a narrow size distribution (relative standard deviation 10−12%). The nanoparticle samples produced with this method contain less than 3% rod-like particles and less than 1% triangular platelets. This is a significant improvement compared to previous methods which produce larger amounts of rod-like particles (5−10%)[35,40] even when CTAB is added.[36,37] Moreover, this experimental implementation based on a one-step procedure allows the reproducible preparation of AuNPs with a predetermined diameter. In fact, accidental loss of material in intermediated purification steps (necessary in multistep procedures) is prevented and the final AuNP size can be precisely defined through calculation of the amount of $HAuCl_4$ solution to be added, knowing the number of inoculated seeds and

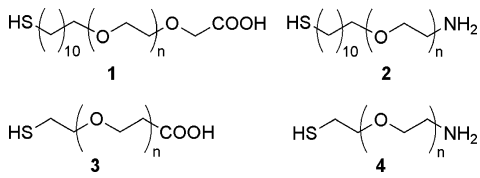

Chart 1. Alkyl-PEG600 thiols (1/2, $n \sim 13$) and PEG3000 thiols (3/4, $n \sim 68$) used for passivation of AuNPs.

their size. We have followed several seeded-growth reactions by withdrawing small samples of the reaction mixture at increasing amounts of added $HAuCl_4$ solution and subsequent analysis *via* scanning electron microscopy (SEM). The standard deviation of the AuNP size distribution of each withdrawn sampled remained constant at approximately 10%, which corresponds to the value measured for the seeds (Figure S-3). This indicates that, under these conditions, no significant particle nucleation occurs during the growth process.[42]

Colloidal Solution Stability of PEG-Passivated AuNPs. To use AuNPs in biological systems, for example, cell cultures, the AuNP colloidal solution must remain stable in a nonaggregated state in the presence of high salt concentrations and possibly high concentration of biomolecules. In fact, nanoparticle stabilization in aqueous solutions is generally achieved with a passivation layer,[43] and PEG-derivatives have proven to be particularly effective. Two classes of PEG thiols have been used: (i) derivatives possessing an alkyl chain between the thiol group and the PEG segment,[44−48] and (ii) derivatives for which the thiol group replaces the terminal hydroxyl of the PEG segment and therefore lacking this additional alkyl chain.[49−53] Nevertheless, to the best of our knowledge, a direct comparison between alkyl-PEG thiols (here represented by derivatives **1** and **2**) and PEG thiols missing such an alkyl chain (Chart 1, **3** and **4**) has not been reported. We have previously described AuNPs passivated with mixed monolayers of PEG thiols belonging to these two classes.[26] The ω-amino terminated thiols **2** and **4** were used to introduce reactive amino groups in the passivation layer of the AuNPs. In that study, we established a method for determining the number of functionalizable amino groups per particle (N_{NH_2}). The results showed no significant difference between the two passivation systems in terms of N_{NH_2}. Moreover, no significant difference in surface coverage between the two systems could be established despite the difference in the average length of the PEG segment ($n \sim 13$ for alkyl-PEG600 derivatives **1**/**2** and ~68 for the PEG3000 derivatives **3**/**4**). We have now extended this preliminary study and, focusing on the applicability of our AuNPs in biological systems, we report here the results of a systematic study on the stability of the AuNPs in high ionic strength solutions and in cell culture medium, specifically comparing these two passivation systems.

Both passivation systems afford AuNPs that do not aggregate when placed in cell culture medium, as shown by UV−vis measurements (Figure S-4). Furthermore, the stability of the colloidal solution in cell culture medium persists for at least 24 h for both systems, as indicated by no significant change in the optical properties of the solutions (Figure S-7). We also investigated the stability of the colloidal solutions with increasing NaCl concentration and as a function of x_{NH_2}, the molar fraction of the amino terminated thiol derivative (**2** or **4**) used during the passivation reaction. This is very important because the number of peptides that can be coupled to the AuNPs depends on x_{NH_2} (*vide infra*). For each AuNP solution measured we determined the aggregation parameter.[18,48] The results of these measurements show that, in the investigated x_{NH_2} range (0.09−0.33), both passivation systems (**1**/**2** and **3**/**4**) effectively stabilize the AuNPs against aggregation with no significant difference (NaCl concentration tested up to 2 M, see Figure S-6). Increasing the amount of ω-amino component **2** or **4** in the passivation reaction beyond $x_{NH_2} = 0.33$ resulted in AuNPs that strongly adhered to glass surfaces and was therefore not further considered.

TABLE 1. Peptide Sequences Used during Conjugation to Passivated AuNPs[a]

	sequence
5	GEγγLQγNQγLIRγKSNC-NH_2
6	GEUULQUNQULIRUKSNC-NH_2

[a] γ = γ-carboxyglutamate, U = γ-glutamate; the side chain of lysine-15 is tetramethylrhodamine labeled in both peptides. Naturally occurring con-G has a sequence corresponding to amino acids 1−17 of **5**.[54]

Conjugation of Peptides to AuNPs. With the aim of developing AuNPs selectively targeting *N*-methyl-D-aspartate (NMDA) receptors, we report here the preparation of several types of conantokin-G (Con-G) functionalized nanoparticles, directly comparing the two introduced passivation systems (alkyl-PEG600 thiols **1**/**2** and PEG3000 thiols **3**/**4**). The coupling strategy, based on a heterobifunctional linker, was previously established by us for AuNPs passivated with a mixture of alkyl-PEG600 thiols.[26] We have varied the AuNP size and the number of amino groups in the passivation layer, thereby controlling the final number of peptides per particle. We also report the coupling of a biologically inactive peptide sequence (Table 1) that we have later used as a control in the cell-culture experiments (*vide infra*).

In parallel to each coupling experiment, we performed a control experiment where the heterobifunctional linker $SM(EG)_2$ (succinimidyl-([*N*-maleimidopropionamido]-diethyleneglycol) ester) was omitted to assess the extent of place-exchange reaction with the PEG thiols of the passivation layer (the peptides carry a Cys-residue) and the presence of unspecific adsorption (see Scheme S-3).

As a starting point, we prepared passivated AuNPs with either alkyl-PEG600 thiols **1**/**2** or with PEG3000 thi-

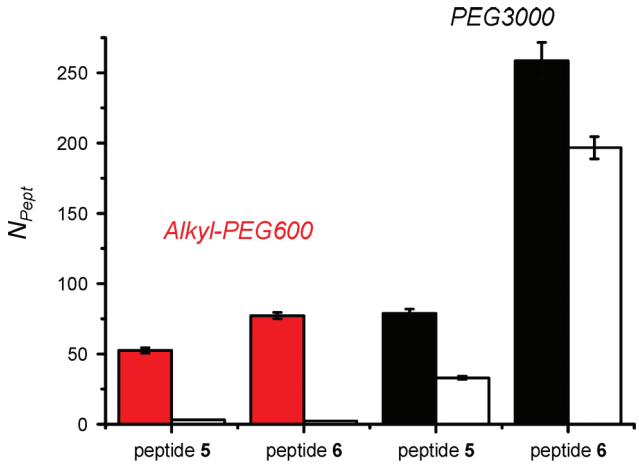

Figure 1. Average amount of peptides per nanoparticle (N_{pept}, AuNP Ø = 32 ± 3 nm). Left: AuNPs passivated with alkyl-PEG600 thiols 1/2. Right: AuNPs passivated with PEG3000 thiols 3/4. x_{NH_2} = 0.14 in all cases. For each peptide, filled columns (red or black) are N_{pept} in the presence of the linker SM(EG)$_2$ and white columns are the corresponding N_{pept} in its absence (place-exchange reaction, see text). Error bars are standard deviation of the measurements.

ols **3**/**4** (both with x_{NH_2} = 0.14) from a single batch of seeded-growth AuNPs (Ø = 32 ± 3 nm). Peptides **5** and **6** were coupled to these passivated particles and the number of coupled peptides per particle (N_{pept}) was measured (Figure 1). For AuNPs passivated with alkyl-PEG600 thiols, N_{pept} is consistent with our previous experiments.[26] Moreover, immobilization of the peptides requires the presence of the heterobifunctional linker SM(EG)$_2$ and no place-exchange or unspecific adsorption was observed, irrespective of the peptide used. In stark contrast, for AuNPs passivated with PEG3000 thiols, a high number of immobilized peptides was also observed in the absence of the heterobifunctional linker SM(EG)$_2$, suggesting a place-exchange reaction.[55]

We have repeated the peptide coupling experiment keeping x_{NH_2} = 0.14 constant for both passivation systems and systematically analyzed AuNPs of different size, from independent seeded-growth batches and from independent passivation reactions. The measured N_{pept} are summarized in Figure 2 (the corresponding numerical values are reported in Table S-2).

Coupling to AuNPs passivated with the alkyl-PEG600 thiols **1**/**2** always resulted in the selective immobilization of the peptides on the passivation layer *via* the heterobifunctional linker SM(EG)$_2$. In fact, the control experiments consistently showed no coupled peptides (N_{pept} = 0 or close to zero) in the absence of the linker.[56] Conversely, coupling to AuNPs passivated with PEG3000 thiols **3**/**4** always resulted in significant peptide immobilization even in the absence of the linker. Moreover, the number of immobilized peptides is quite variable and most likely depends on the extent of the place-exchange reaction taking place for a particular

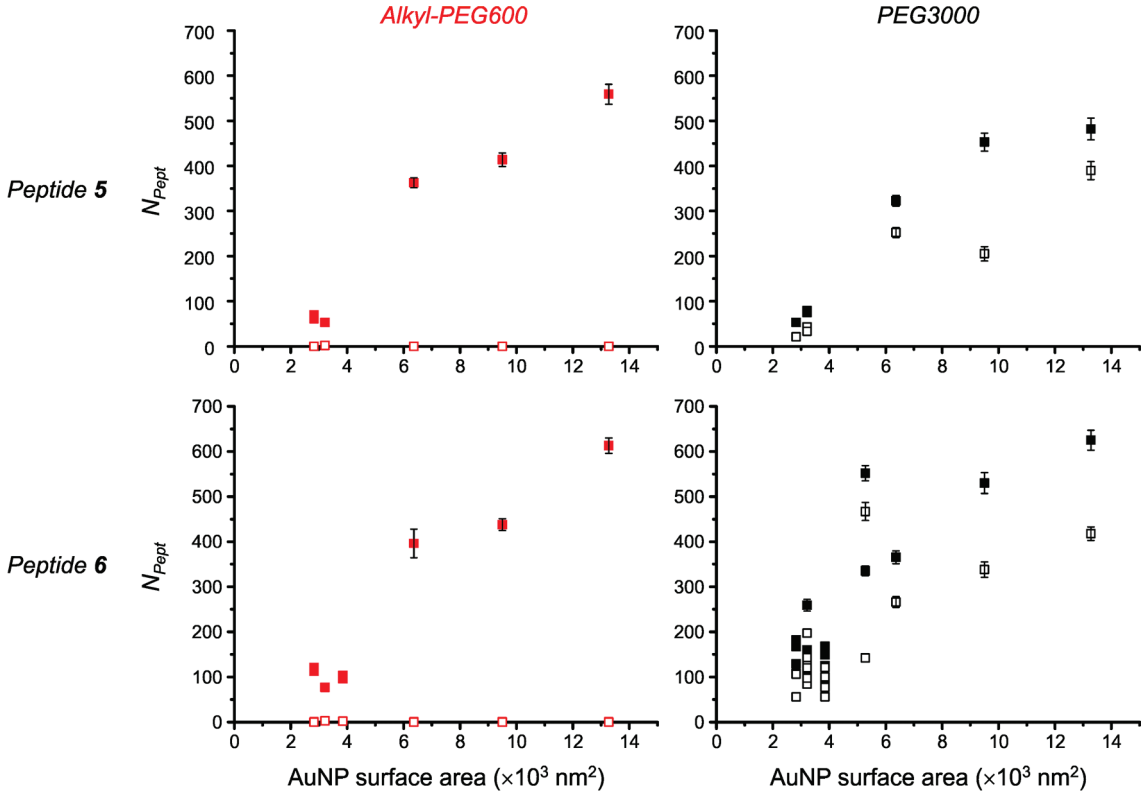

Figure 2. Average amount of peptides per nanoparticle (N_{pept}) as a function of the AuNP surface area. Left: AuNPs passivated with alkyl-PEG600 thiols 1/2. Right: AuNPs passivated with PEG3000 thiols 3/4. x_{NH_2} = 0.14 in all cases. For each peptide (5 or 6), solid symbols (red or black) are N_{pept} values obtained in the presence of the linker SM(EG)$_2$ and open symbols are N_{pept} values obtained from the control experiments where the linker was omitted. Error bars are the standard deviation of the measurements.

AuNP sample. Nevertheless, it is important to realize that in every case the extent of the place-exchange reaction is far below complete replacement of the PEG3000 thiols. Based on previous data, the fraction of exchanged thiols is in fact estimated to be below 10% (PEG3000 thiols per 30 nm-AuNP: ~2800).[26]

We also investigated the stability of the colloidal solutions of these peptide-functionalized AuNPs under conditions analogous to those reported for only passivated AuNPs, that is, in cell culture medium and at increasing NaCl concentrations. Again, we observed no difference in stability between the two passivation systems irrespective of the conjugated peptide (**5** or **6**, see Figures S-5 and S-6). Furthermore, these peptide-functionalized AuNPs are as stable as the only passivated AuNPs. This suggests that the PEG layer dictates predominantly the stability of the colloidal solution even for AuNPs where a small fraction of thiols have been exchanged (PEG3000 passivation system). Yet, we have shown above that the two passivation systems definitely behave differently at the molecular level.

As discussed above, peptides are immobilized on AuNPs passivated with PEG3000 thiols even in the absence of the heterobifunctional linker $SM(EG)_2$ and this is attributed to a measurable extent of place-exchange reaction. For the reaction to occur, the peptides must diffuse through the passivation layer to reach the gold surface. Both peptides **5** and **6** have hydrophilic, negatively charged sequences. We, therefore, speculate that diffusion of the peptides through the passivation layer may be slowed down for the alkyl-PEG600 system (**1**/**2**) compared to the PEG3000 system (**3**/**4**) as a result of the hydrophobic alkyl chains, resulting in improved shielding of the AuNP surface. For the PEG3000 passivation system, it should however be possible to prevent the place-exchange reaction, increasing the steric hindrance of the incoming thiol, thereby restraining its diffusion through the passivation layer. Thus, by taking an "infinitely large" thiol, immobilization should only occur *via* the maleimide residues as in the case of the alkyl-PEG600 system. To test this hypothesis, a sample of PEG3000 passivated AuNPs ($x_{NH_2} = 0.14$) was split in two and one aliquot was functionalized with the heterobifunctional linker $SM(EG)_2$, while the other remained unfunctionalized. The AuNPs were then incubated with commercially available thiol-functionalized magnetic beads (0.7−1.4 μm, the "infinitely large" thiol). After washing, the samples were imaged by SEM. Clearly AuNPs were immobilized on the micro bead surface only if they had been functionalized with the linker and therefore carried maleimide residues (Figures S-10a *vs* S-10b). Hence, if the incoming thiol is not allowed to diffuse through the passivation layer, here for steric reasons, no place-exchange reaction takes place and no AuNPs are immobilized in the absence of the linker. This experiment strongly supports the hypothesis that the immobilization of peptides on AuNPs passivated with PEG3000 thiols in the absence of the linker is indeed due to place-exchange.

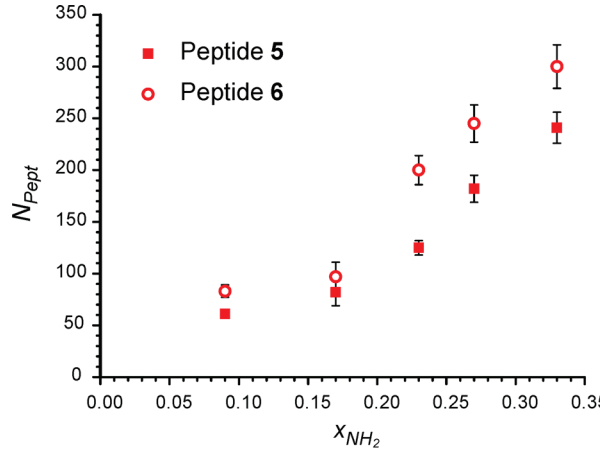

Figure 3. Average amount of coupled peptides per nanoparticle (N_{pept}) as a function of x_{NH_2} for AuNPs passivated with alkyl-PEG600 thiols 1/2, Ø = 30 ± 3 nm. Error bars are standard deviation of the measurements.

The concomitant occurrence of place-exchange and linker-mediated peptide immobilization observed for AuNPs passivated with PEG3000 thiols **3**/**4** precludes the possibility of controlling the number of coupled peptides under our experimental conditions. On the other hand, the selective linker-mediated peptide immobilization observed for AuNPs passivated with alkyl-PEG 600 thiols **1**/**2** should allow control of N_{pept} by varying the number of functionalizable amino groups N_{NH_2} in the passivation layer. To test this, AuNPs were passivated with alkyl-PEG600 thiols **1**/**2** at increasing x_{NH_2}, which in turn resulted in increased N_{NH_2}. Subsequent functionalization with peptides **5** and **6** showed that N_{pept} also linearly increased with x_{NH_2} (see Figure 3 and Table S-3).

Binding of ConG Functionalized AuNPs to NMDA Receptors. NMDA receptors are glutamate-gated ion channels with high permeability for calcium in the mammalian central nervous system.[57−60] The peptide-toxin ConG[54] is a well-known NMDA receptor antagonist with high selectivity for receptors containing the subunit NR2B.[61,62] Because of its subunit selectivity, the 17-amino acid long peptide ConG is a very interesting and promising drug candidate for the treatment of diseases related to NMDA malfunctioning.[63,64] The way ConG affects the activity of NMDA receptors has been studied intensively at the cellular level.[62,65−67] A widely used *in vitro* model system is based on HEK 293 cells, which recombinantly express the NMDA receptors.[68,69] This system is very well established and was reported in 1992 in conjunction with the cloning of the NMDA receptor subunits NR2A, NR2B, and NR2C from rat brain.[70] Thus, for further investigations with ConG-functionalized AuNPs, we chose HEK 293 cells transiently expressing NMDA receptors comprising the NR1a and NR2B subunits. We then addressed three main questions: (i) if ConG-functionalized AuNPs selec-

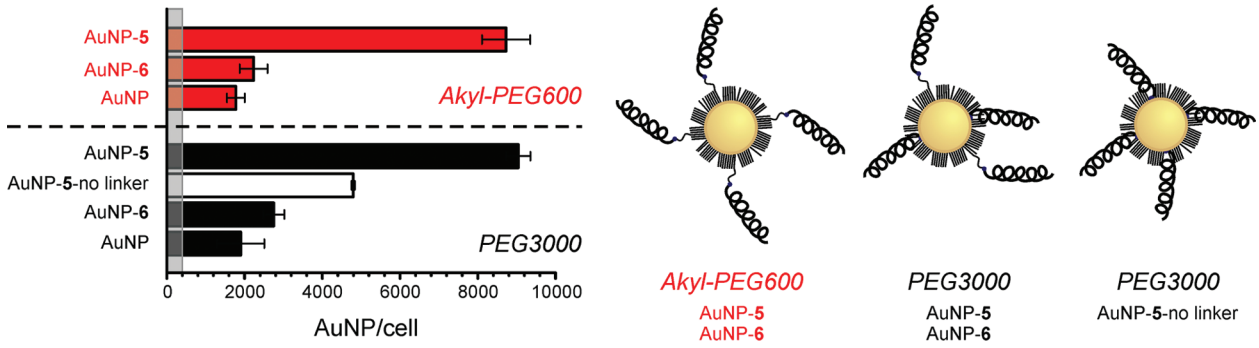

Figure 4. Selective binding of AuNPs functionalized with peptide 5 (AuNP-5, ConG sequence) to HEK 293 cells expressing NMDA receptors (NR1a/NR2B, transfection efficiency ~50%). AuNP-6, particles functionalized with the mock-peptide 6; AuNP, passivated AuNPs, no coupled peptides; AuNP-5-no linker, $SM(EG)_2$ omitted during coupling, peptides are directly immobilized on the Au surface (only for PEG3000 passivation system, see text). AuNP diameter Ø = 29 ± 3 nm. Alkyl-PEG600 passivation system (1/2): x_{NH_2} = 0.14; N_{pept}, 76 ± 5 (AuNP-5); 63 ± 9 (AuNP-6). PEG3000 passivation system (3/4): x_{NH_2} = 0.14; N_{pept}, 91 ± 14 (AuNP-5); 62 ± 20 (AuNP-6); 100 ± 22 (AuNP-5-no linker). The gray area (~400 AuNP/cell) represents the limit of detection for the assay. Error bars are standard deviations of three independent experiments.

tively bind to NMDA receptors; (ii) if the affinity for the receptor is affected (and to what extent) by the multivalent nature of our AuNPs-peptide conjugates; and (iii) if the topological localization of the immobilized peptide on the AuNP surface, that is, on the passivation layer as opposed to within the passivation layer (Figure 4), affects binding.

Transfected HEK 293 cells were incubated with the required AuNP solution in cell culture medium for 30 min. Subsequently, cells were washed, suspended by trypsinization, and counted. The total content of gold in the sample was determined by ICP-OES after treatment with *aqua regia*. The average number of AuNPs per cell was calculated from the amount of gold and the number of cells in the sample. For both passivation systems (alkyl-PEG600 thiols **1**/**2** and PEG3000 thiols **3**/**4**) we considered AuNPs functionalized with peptide **5** (ConG sequence) *versus* AuNPs functionalized with the biologically inactive peptide **6** (mock-peptide). Simply passivated AuNPs were taken as a control. Importantly, all AuNPs had the same size and a comparable number of N_{pept} (Figure 4).

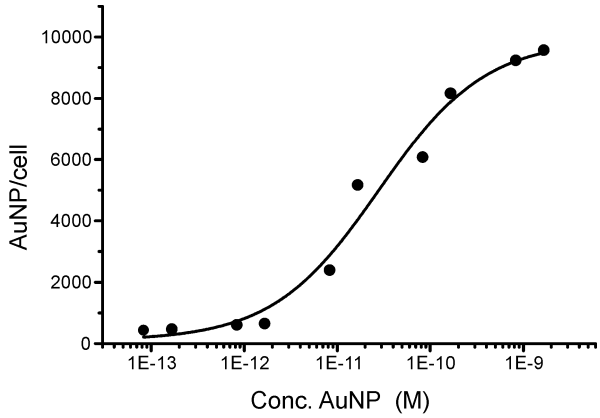

Figure 5. Binding curve for AuNPs (Ø = 29 ± 3 nm) functionalized with peptide 5 (ConG sequence) to NMDA receptors expressed by HEK 293 (NR1a/NR2B receptor subunits, transfection efficiency ~50%). Alkyl-PEG600 passivation system: thiols 1/2 x_{NH_2} = 0.14; average number of peptides per AuNP, 80 ± 5.

AuNPs carrying peptide **5** (ConG sequence) always bind in significantly higher number to the cells (8620 ± 630 AuNP/cell for alkyl-PEG600 and 8930 ± 350 AuNP/cell for PEG3000 passivation) compared to AuNPs functionalized with the mock peptide **6** (≤2700 AuNP/cell) or only passivated AuNPs (≤1900 AuNP/cell). These background levels may possibly originate from incomplete removal of the unbound AuNPs. The typically not strongly adhering HEK293 cells must be rinsed very gently to avoid detaching them from the support. Therefore, AuNPs that are loosely and unspecifically attached to the cell membrane, within folds and wrinkles, or even on the bottom of the Petri dish could possibly not be completely washed out in the three rinsing steps. On the other hand, we cannot completely exclude that a small fraction of the number of particles per cell may be the result of cellular uptake (generally *via* endocytosis for particles of this size).[71] It is however known that cellular uptake strongly depends on the surface characteristics of the AuNPs.[72] Therefore, this contribution is most likely small since the AuNPs used for the two controls give substantially the same background values although differing in surface functionalization (AuNPs with mock peptide or simply passivated AuNPs). Furthermore, it was clearly shown that PEGylated AuNPs are not, or only minimally, internalized even after several hours incubation with cells,[11,21,73] while in our case the incubation time is restricted to 30 min. Finally, it is worth noticing that the comparison with AuNPs functionalized with the mock peptide **6** allows emphasis of the specificity of the interaction between the NMDA-receptors and the AuNPs carrying the correct ConG sequence (**5**) and minimizes any unspecific contribution. Similar binding for alkyl-PEG600 AuNP-**5** and PEG3000 AuNP-**5** is not surprising because both possess fully exposed peptides. In addition, PEG3000 AuNP-**5** conjugates display peptides within the passivation layer, which bind with lower affinity (*vide infra*). Unfortunately, it is not possible to give a reliable estimate of the relative amount of peptides

within the passivation layer *versus* peptides on the surface of the passivation. In fact, the variations in the extent of place-exchange reaction are comparable to the number of meleimide-coupled peptides (Figure 2).

We also investigated samples of PEG3000 passivated AuNPs functionalized with ConG peptides prepared by omitting the heterobifunctional linker $SM(EG)_2$ during the coupling step (indicated as AuNP-**5**-no linker). In this case, as discussed above, the peptides are immobilized *via* place-exchange reaction and therefore reside *only* within the passivation layer. In contrast, AuNP-**5** with alkyl-PEG600 thiols carry peptides immobilized only on the solvent-exposed interface of the passivation layer. Comparison of these two systems shows a significantly reduced number of particles per cell for the AuNP-**5**-no linker system (4730 ± 140 AuNP/cell), despite the N_{pept} for the two AuNP samples being practically identical (100 ± 22 *vs* 91 ± 14). This result confirms the validity of our design, directly proving that optimal interaction between a biologically active peptide and a cell-membrane receptor can be achieved by immobilization of the peptide at the solvent-exposed interface of the passivation layer. Furthermore, for the alkyl-PEG600 passivated AuNP-**5**, we determined the binding strength between the nanoparticles and the NMDA receptors. HEK 293 cells expressing NMDA receptors were incubated with increasing nanoparticle concentrations. For each sample we performed the binding assay reported above to quantify the number of AuNP per cell. The results, plotted as a function of AuNP concentration, gave a well-defined binding curve from which the dissociation constant could be estimated as $K_{D\text{-}AuNP} = (2.8 \pm 1.0) \times 10^{-11}$ M (Figure 5). Because the AuNPs used in this experiment (Ø = 29 ± 3 nm) carry 80 ± 5 copies of peptide **5** per particle, the apparent dissociation constant for the ConG peptide, when conjugated to the AuNPs, is $K_{D\text{-}ConG} = (2.2 \pm 0.8) \times 10^{-9}$ M. By comparison, the binding affinity for soluble ConG, determined in a very similar HEK 293 cell system, was found to be 2.3 μM.[65] This large increase in binding affinity of approximately 10^3 times is a direct consequence of the multivalency[28] of these AuNPs and indicates that even in the case of relatively weak ligand−receptor interaction, efficient receptor targeting can be reached with low AuNP concentrations (below 1 nM). While for labeling purposes, such as immunogold labeling, a relatively low binding efficiency can still be acceptable and unproblematic,[74,75] multivalent, strongly binding AuNPs, such as those described here, are certainly advantageous for the development of functional nanomaterials, where for instance a biological function can be elicited by binding of a functionalized AuNP.

The specific binding of the AuNPs functionalized with peptide **5** on the cell membrane of HEK 293 cells expressing NMDA receptors was also confirmed *via* SEM analysis. Based on the binding data described above, cells were incubated with AuNPs passivated with alkyl-PEG600 thiols functionalized either with the biologically active peptide **5** or with the mock peptide **6** at an AuNP concentration of 0.17 nM, corresponding to 1×10^{11} part/mL. Under these experimental conditions, approximately 80% of the NMDA receptors in our system can be targeted. The samples were then washed, fixed, and prepared for imaging. Cells incubated with the AuNP-**5** conjugate show a high number of AuNPs on their cell-membrane surface (Figure 6a), while we were not able to find particles bound to cells in the case of the AuNP-**6** conjugate (Figure 6b). Nevertheless, during the binding assay reported above (Figure 4) we could detect a relatively small number of AuNPs per cell for both only passivated AuNPs (≤1900 AuNP/cell) and AuNPs-**6** (≤2700 AuNP/cell). These background levels are probably due to residual unspecific binding (*e.g.*, to the extracellular matrix) or to cellular uptake and can be quantitatively appreciated only by the binding assay carried out on a whole cell population and not by SEM imaging. Taken together these results definitely prove that the ConG sequences immobilized on our AuNPs are recognized by the NMDA receptors on the membrane of HEK 293 cells with high specificity.

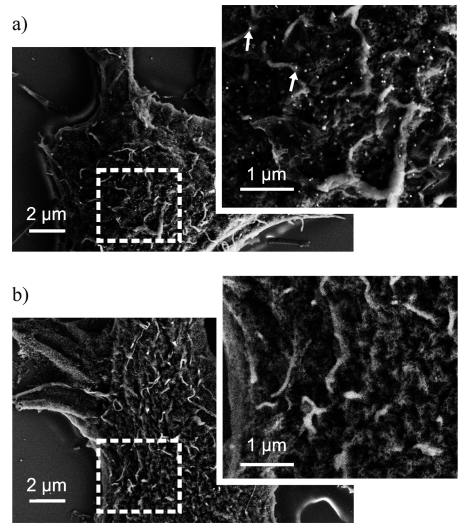

Figure 6. SEM micrographs showing the selective binding of AuNPs (Ø = 29 ± 3 nm) functionalized with peptide 5 (ConG sequence) to HEK 293 cells transfected with NMDA receptors (NR1a/NR2B, transfection efficiency ~50%). Alkyl-PEG600 passivation system: thiols 1/2 x_{NH_2} = 0.14, average number of peptides per AuNP: (a) AuNP-5: 80 ± 5; (b) AuNP-6: 62 ± 5.

CONCLUSIONS

In this study we have reported the preparation of PEG-passivated AuNPs functionalized with a precise number of biologically active peptides. The aim of this paper was, first of all, to show a direct comparison between two widely used PEG-thiol-based passivation systems. One system consists of derivatives with a C_{11}-alkyl chain between the thiol group and the PEG segment and is here represented by alkyl-PEG600 thiols **1**/**2**. The other consists of derivatives with a thiol-

terminated PEG chain, in this study, PEG3000 thiols **3**/**4**. Although both systems result in an equally good stabilization of the colloidal AuNP solutions in media of high ionic strength, we showed that the two systems behave differently during conjugation of Cys-terminated peptides *via* an NHS-maleimido heterobifunctional linker. No concomitant place-exchange reaction was observed for AuNPs passivated with thiols **1**/**2**. In contrast, this reaction took place to a small but measurable extent for AuNPs passivated with thiols **3**/**4** and a considerable number of peptides were immobilized on the nanoparticles even in the absence of the linker. As a consequence, precise control over the number of coupled peptides per particle is only possible with the passivation system based on thiols **1**/**2**. Additionally for this system, the peptides are coupled only to the solvent-exposed interface of the passivation shell and we demonstrate here that this allows optimal interaction between the AuNPs and receptors on the cell surface. Taking AuNPs functionalized with peptide **5** (ConG sequence) and HEK 293 cells expressing NMDA receptors, we have established a binding assay to determine the average number of AuNPs per cell. We have compared AuNPs carrying the peptides only on the passivation layer (AuNP-**5**, alkyl-PEG600 system) with AuNPs carrying the peptides only on the gold surface, that is, within the passivation layer (AuNP-**5**-no linker, PEG3000 system). For the first system, a significantly higher number of AuNPs per cell was observed, confirming the higher accessibility of the peptides. Finally, we have measured a 10^3 times increase in binding affinity for the AuNP-coupled peptide (AuNP-**5**, alkyl-PEG600 system, $N_{pept} = 80 \pm 5$) compared to the free peptide in solution. This result shows that, even in the case of relatively weak ligand−receptor interactions (K_D in the μM range), high affinity AuNP probes can be developed as a result of the multivalent nature of these objects. The AuNP preparation strategy reported in this paper, in conjunction with the distinctive characteristics of the passivation system based on alkyl-PEG600 thiols **1** and **2**, allows direct and quantitative control of the multivalent nature of the AuNPs. Conjugation of peptide-based NMDA receptor antagonists to AuNPs could be used to spatially restrict NMDA-receptor-blockade to specific cellular locations and may be suitable to specifically block extrasynaptic NMDA receptors that promote cell death pathways and neurodegeneration.[76] We are currently investigating the targeting of functionalized AuNPs to other relevant cell surface receptors and progress in this direction will be reported in due course.

METHODS

Materials. All reagents used were purchased from Sigma-Aldrich, Fluka, or Acros Organics, unless mentioned otherwise, and used without further purification. 5(6)-Carboxyfluorescein was purchased from Novabiochem. The heterobifunctional linker succinimidyl-([*N*-maleimidopropionamido]-diethyleneglycol) ester ($SM(EG)_2$) was obtained from Pierce and dithiothreitol (DTT) was obtained from Serva. PEG3000 thiols **3** and **4** were purchased from RAPP Polymere GmbH (Tübingen, Germany). Peptide **5** (sequence: GEγγLQγNQγLIRγK(TAMRA)SNC-NH_2; γ = gamma-carboxy glutamate, TAMRA = tetramethylrhodamine) was purchased in a custom synthesis from PSL-Peptide Specialty Laboratories (Heidelberg, Germany). Peptide **6** (sequence: GE-UULQUNQULIRUK(TAMRA)SNC-NH_2; U = gamma glutamate) was purchased in a custom synthesis from Biosyntan (Berlin, Germany). For the coupling experiments, dimethylformamide with certified low free-amine content was used (DMF: peptide synthesis quality, Fluka). Dulbecco's Modified Eagle Medium (DMEM), 0.05% trypsin/EDTA, and fetal bovine serum (FBS) were purchased from Gibco, paraformaldehyde (16% in methanol) from Alfa Aesar, glutaraldehyde (25%) for electron microscopy from Merck, poly-L-lysine (0.1% w/v in water) from Sigma, propidium iodide (PI; 1 mg/mL) from Sigma Aldrich, lipofectamine 2000 from Invitrogen, NR1 antibody (MAB1586) from Millipore, and Anti-Mouse IgG (whole molecule)−R-Phycoerythrin antibody from Sigma. All glassware employed for nanoparticle preparation and storage was cleaned with aqua regia (HCl (37%)/HNO_3 (65%) 3:1). Ultrapure deionized water (TKA GenPure water purification system, 18.2 MΩ cm) was used for the preparation of all aqueous solutions. All solutions used for nanoparticle preparation were filtered through a 0.2 μm membrane filter (Whatman). Ultrafiltration of nanoparticle samples was carried out on Amicon Ultra-4 Centrifugal Filter Unit, regenerated cellulose, 100 kDa from Millipore; gel filtration on NAP-10 columns from GE Healthcare.

Instrumentation. The size of the gold nanoparticles was analyzed *via* SEM (Zeiss, Ultra 55 equipped with a Gemini gun, 5−10 kV) or TEM (Philips CM 200, 200 kV). UV/vis spectra and fluorescence measurements were carried out using a TEKAN Infinite M200 plate reader. The concentration of gold was determined *via* ICP-OES (Spectro, CIROS CCD) or AA (Perkin-Elmer, PE 5000). NMR spectra were recorded on a Bruker AMX-300 spectrometer. ^{1}H NMR spectra were calibrated to TMS on the basis of the relative chemical shift of the solvent as an internal standard. MALDI-TOF mass spectra were recorded on a Bruker BIFLEX III spectrometer.

AuNP Seeded-Growth. AuNP seeds (15 mL, 6.5 nM, 12−14 nm diameter[41]) were added to an aqueous solution of hydroxylamine hydrochloride (180 mL, 10 mM). An aqueous solution of $HAuCl_4$ (255 mL, 0.65 mM) was added at constant flow (50 mL/h, KD Scientific syringe pump) while the receiving solution was continuously stirred with a magnetic stirrer. After addition was completed, the resulting deep red solution was centrifuged (40 min, 4160 × g), the supernatant was discarded, and the AuNPs were resuspended in 9 mL water. Figure S-1 shows the development of the AuNP size upon addition of $HAuCl_4$ in one of these seeded-growth reactions.

Synthesis of Alkyl-PEG600 Thiols 1 and 2. Thiolated PEG derivatives carrying an alkyl chain between the sulfhydryl group and the ethylene glycol chain were prepared according to the synthetic strategy developed by the Whitesides' group,[77,78] with additional steps allowing for the introduction of ω-carboxyl[46,79,80] and ω-amino groups.[81] Notably, thiol derivatives **1** and **2** are not commercially available. They are not single compounds, but mixtures of homologous compounds, because the PEG segment comes from a mixture of oligomers whose chains are on average 13 ethylene glycol units long (PEG600). While taking PEG600 as the starting material may be regarded as introducing additional difficulties during purification compared to a single PEG compound, it has the advantage of being an inexpensive source of medium length PEG chains. The complete synthetic strategy (Schemes S-1 and S-2) and the characterization of each intermediate are reported in the Supporting Information.

Passivation of the AuNPs. Typical passivation reactions were carried out by adding the AuNPs to an aqueous solution containing $NaHCO_3$ and a mixture of amino- and carboxy-terminated thiols (**1**/**2** or **3**/**4**) with the desired molar fraction of amino-terminated derivative ($0.09 \leq x_{NH_2} \leq 0.33$). Stock solutions of thiols in EtOH (5 mM) were freshly prepared and directly used or used within a few days, during which they were stored at −20 °C. Final reaction volume was typically 1.75 mL, and final concentrations were AuNPs 1−5 nM, $NaHCO_3$ 25 mM, and total thiols (**1** + **2** or **3** + **4**) 1 mM, and therefore, the reaction mixtures contained 20% volume of EtOH. Stirring at rt was continued for 48−72 h after which AuNPs were purified by ultrafiltration using Amicon Ultra 4 centrifugal filter units (1 × 4 mL H_2O, 4 × 4 mL EtOH/40 mM $NaHCO_3$ buffer pH 8.4 (2:8) and 3 × 4 mL 40 mM $NaHCO_3$ buffer) followed by gel filtration on NAP-10 columns (elution with 40 mM $NaHCO_3$ buffer).

Salt Aggregation Tests and Stability in Cell Culture Medium. The tests were carried out in a 96-microtiter plate, with a 200 μL final volume per well. Aliquots (10 μL) of AuNP colloidal solution (4 nM) were pipetted into the necessary amount of water and then increasing volumes of a 3 M NaCl stock solution were added. The solutions were shaken vigorously and incubated for 30 min before measuring the UV−vis spectra. The final NaCl concentrations were 0.4, 0.8, 1.2, 1.6, and 2.0 M. Alternatively, 10 μL aliquots of AuNPs colloidal solution (4 nM) were diluted to 200 μL with cell culture medium (DMEM, without phenol red). UV−vis spectra were recorded every 30 min for 12−24 h.

Coupling of Peptides 5/6 (Scheme S-3). The experimental procedure for coupling peptides to PEG-passivated AuNPs has already been reported.[26]

Coupling of AuNPs to Thiol-Functionalized Magnetic Beads. Thiol-functionalized magnetic beads (MagSi-Tools 1.0 from Magna-Medics) were pretreated following the procedure described by the manufacturer. AuNPs passivated with PEG3000 thiols **3**/**4** (50 μL, ∼1−5 nM in 100 mM sodium phosphate buffer, pH 7.0) were functionalized by the addition of $SM(EG)_2$ linker solution (5 μL, 50 mM in DMF) and shaken 2 h at 4 °C. Purification of the linker functionalized AuNPs was performed *via* ultrafiltration followed by gel filtration eluting with water. The resulting AuNP solution was incubated overnight with the magnetic beads at 4 °C. The beads were repeatedly washed with 40 mM $NaHCO_3$ (7×), transferred on a silicon wafer and imaged by SEM. A second AuNP aliquot was treated in parallel in the same way, however, omitting the linker. These AuNPs remained therefore unfunctionalized and were used as a control.

HEK 293 Cell Culture. HEK 293 cells (DSMZ, Braunschweig) were cultured in DMEM with 10% FBS (called in the following paragraphs "culture medium") at 37 °C/5% CO_2 and passaged every 2−3 days.

Optimized Transfection Protocol. A total of 24 h after having seeded the cells, the standard culture medium was replaced with 2 mL of DMEM containing 500 μM of DL-2-amino-5-phosphonopentanoic acid (APV). For transfection, two solutions were prepared separately: (a) 10 μL of lipofectamine 2000 were diluted in 100 μL of DMEM and (b) plasmids (4 μg each of the two plasmids encoding the receptor subunits NR2B and NR1a) were dissolved in 100 μL of DMEM. After 5 min, the two solutions were combined and incubated at rt for 20 min. Subsequently, this solution was added slowly to the cells (the reported amount is used for each well of a six-well plate), mixed gently, and incubated for 3 h at 37 °C/5% CO_2. Afterward, the medium was replaced with 3 mL of cell culture medium containing 500 μM APV and kept at 37 °C/5% CO_2 for 24 h. The conditions reported above represent the best conditions found compromising between cell viability and transfection efficiency.

Cell Counting. The number of living cells was determined 24 h after transfection. Cells were washed with cell culture medium (2 × 2 mL) and with PBS (1 × 2 mL) to remove dead cells and then trypsinized with 700 μL of trypsin/EDTA at 37 °C/5% CO_2 for 2 min. After standard washing and resuspension, cells were counted using a Z2 Coulter Particle Count and Size Analyzer.

Flow Cytometric Analysis for Determination of Transfection Efficiency. A total of 24 h after transfection, cells were washed and trypsinized as reported above, dispersed in PBS (1 × 10^6 cells/mL), and then analyzed *via* flow cytometry using a Beckman Coulter, cytomics FC 500 instrument. Positively transfected cells were identified by the GFP fluorescence signal, which originates from expression of the NR2B subunit-GFP fusion protein. In parallel, to determine the amount of nonviable cells, propidium iodine (PI; 20 μL, 0.5 μg/μL) was added to 1 mL of cell suspension in PBS, incubated for 15 min, and measured.

Antibody Labeling of Cells Transfected with cDNA Encoding the NR1a Receptor Subunit. Recombinant expression of the NR1a receptor subunit after transfection was confirmed by antibody labeling [primary antibody: anti-NMDAR1, all splice variants, clone R1JHL from Millipore (MAB1586); secondary antibody: Anti-Mouse IgG (whole molecule)−R-Phycoerythrin antibody from Sigma]. The labeling procedure was performed following the instruction described by the manufacturer (Fix and Perm reagents, Invitrogen). Shortly, transfected cells were tripsinized, washed and resuspended. For fixation, 5 × 10^5 cells were resuspended in 100 μL of fixation solution and incubated for 15 min at room temperature. Afterward, 3 mL of PBS (5% FBS) were added, and the cell suspension was centrifuged for 5 min at 300 × g. The supernatant was removed and cells were resuspended in 100 μL of permeabilization reagent and mixed gently. The primary antibody (300 μL; 1:1000) was added and incubated with the cells for 15 min at rt. The cell suspension was then added of 3 mL of PBS (5% FBS) and centrifuged for 5 min at 300 × g. The cell pellet was then taken up in a mixture of 100 μL of permeabilization reagent containing the PE-conjugated secondary antibody (1:600) and 500 μL of PBS. The suspension was incubated for 20 min at rt in the dark and then diluted with 3 mL of PBS (5% FBS). The cells were again centrifuged (5 min, 300 × g) and resuspended in PBS for flow cytometry analysis.

Binding Assay (Scheme S-4). HEK 293 cells were transfected with cDNAs encoding the NR2B/NR1a receptor subunits and cultured for 24 h at 37 °C/5%CO_2, as described above. The transfected cells were then washed with culture medium (2 × 2 mL) and with PBS (1 × 2 mL) to remove dead cells and the NMDA receptor antagonist APV. The AuNP samples were pipetted onto the cells (1 × 10^{11} AuNPs in 50 μL of 40 mM $NaHCO_3$ buffer diluted within 700 μL of culture medium) and incubated for 30 min at 37 °C/5% CO_2. Subsequently, the fluid was aspirated and the cells were washed with culture medium (2 × 2 mL) and with PBS (1 × 2 mL) to remove unbound AuNPs. The cells were then trypsinized with 700 μL of trypsin/EDTA for 2 min. A total of 1 mL of culture medium was added, and the suspension was transferred in a 15 mL Falcon tube followed by an additional 1 mL portion of cell culture medium used to rinse the well. The suspension was shortly vortexed to make it homogeneous and a 100 μL aliquot was withdrawn to determine the total number of cells. The rest of the suspension was centrifuged for 45 min at 4160 × g to ensure complete AuNPs sedimentation. The supernatant was discarded and the cell/AuNPs pellet was treated with 0.5 mL of concd HCl and 0.25 mL of concd HNO_3. After a 1 h digestion, the solution was quantitatively transferred into a 10 mL volumetric flask and made up with Milli-Q water to the final volume. The amount of gold in this solution was determined by ICP-OES analysis. The detection limit for the gold content measurements (three times the standard deviation of the baseline) corresponds to 0.05 μg/mL. Because the number of cells used in a binding assay is ∼1 × 10^6 cells and the used AuNPs had a diameter of 29 nm, the limit of detection for the assay corresponds to ∼200 AuNP/cell. However, to account for the variation in the number of cells between different samples, we have taken 400 AuNPs/cell as a more conservative estimate of the limit of detection (Figure 4).

Determination of the Binding Affinity of Peptide-Conjugated AuNPs. Peptide **5** (ConG sequence) was conjugated to alkyl-PEG600 passivated AuNPs (Ø = 29 ± 3 nm, thiols **1**/**2** x_{NH_2} = 0.14), as reported above. The number of conjugated peptides was determined: N_{pept} = 80 ± 5. Samples of HEK 293 cells recombinantly expressing NMDA receptors (NR2B/NR1a transfection efficiency ∼50%) were incubated with AuNP-**5** dissolved in 200 μL of 40 mM $NaHCO_3$ and 700 μL of culture medium for 30 min. The nanoparticle concentration was varied in the interval 1 × 10^{12}−5 × 10^7 particles/mL, which corresponds to 1.66−8.30 × 10^{-5} nM. To determine the average number of AuNPs per cell, each

cell sample was further treated as described for the binding assay.

Cell Preparation for SEM Imaging. Cells samples on poly-L-lysine coated glass coverslips were incubated with the desired peptide conjugated AuNPs (AuNP-**5** or AuNP-**6**) for 30 min. Unbound AuNPs were washed with PBS and cells were fixed with 4% paraformaldehyde and 1.5% glutaraldehyde in 0.1 M cacodylate buffer for 2 h. Dehydration of the cells was performed with successive washing steps of increasing EtOH concentration (20−100% EtOH in water) followed by critical point drying (Bal-Tec critical point dryer, CPD 030) and carbon coating (Bal-Tec MED 20 coating system). Prepared samples were then imaged *via* SEM.

Acknowledgment. The authors thank Mr. Albrecht Meyer and Mr. Gerhard Werner (ZWE-Analytische Chemie, MPI for Metals Research, Stuttgart) for the ICP-OES and AA measurements, Prof. Andres Jäschke and Mr. Heiko Rudy (IPMB, University of Heidelberg) for the MALDI-TOF measurements, Mr. Arthur Lint for the synthesis of some PEG derivatives, Dr. Georg Köhr (MPI for Medical Research, Heidelberg) for the plasmid of the NR1a subunit, and Dr. Daniela Mauceri (IZN, University of Heidelberg) for the plasmid of the NR2B subunit. The authors also thank Dr. Richard Segar for proof-reading the manuscript. L.M. acknowledges the Studienstiftung des Deutschen Volkes (Germany) for a fellowship. The Max Planck Society is acknowledged for financial support. This work was supported by the Excellence Cluster *CellNetworks* at the University of Heidelberg.

Supporting Information Available: SEM/TEM determination of the AuNP size; synthesis and characterization of alkylPEG600 derivatives; analysis of the stability of the AuNP colloidal solutions; average number of peptides per particle (N_{pept}) for all AuNP samples; SEM images of thiol-functionalized magnetic beads incubated with AuNPs; flow cytometry measurements; and schematic representation of the assay for the quantitative determination of the average number of bound AuNPs per cell (binding assay). This material is available free of charge *via* the Internet at http://pubs.acs.org.

REFERENCES AND NOTES

1. De, M.; Ghosh, P. S.; Rotello, V. M. Applications of Nanoparticles in Biology. *Adv. Mater.* **2008**, *20*, 4225–4241.
2. Rosi, N. L.; Mirkin, C. A. Nanostructures in Biodiagnostics. *Chem. Rev.* **2005**, *105*, 1547–1562.
3. Alivisatos, P. The Use of Nanocrystals in Biological Detection. *Nat. Biotechnol.* **2004**, *22*, 47–52.
4. Boisselier, E.; Astruc, D. Gold Nanoparticles in Nanomedicine: Preparations, Imaging, Diagnostics, Therapies and Toxicity. *Chem. Soc. Rev.* **2009**, *38*, 1759–1782.
5. Murphy, C. J.; Gole, A. M.; Stone, J. W.; Sisco, P. N.; Alkilany, A. M.; Goldsmith, E. C.; Baxter, S. C. Gold Nanoparticles in Biology: Beyond Toxicity to Cellular Imaging. *Acc. Chem. Res.* **2008**, *41*, 1721–1730.
6. Sperling, R. A.; Rivera Gil, P.; Zhang, F.; Zanella, M.; Parak, W. J. Biological Applications of Gold Nanoparticles. *Chem. Soc. Rev.* **2008**, *37*, 1896–1908.
7. Chen, P. C.; Mwakwari, S. C.; Oyelere, A. K. Gold Nanoparticles: from Nanomedicine to Nanosensing. *Nanotechnol., Sci. Appl.* **2008**, *1*, 45–66.
8. Baptista, P.; Pereira, E.; Eaton, P.; Doria, G.; Miranda, A.; Gomes, I.; Quaresma, P.; Franco, R. Gold Nanoparticles for the Development of Clinical Diagnosis Methods. *Anal. Bioanal. Chem.* **2008**, *391*, 943–950.
9. Pujals, S.; Bastus, N. G.; Pereiro, E.; Lopez-Iglesias, C.; Puntes, V. F.; Kogan, M. J.; Giralt, E. Shuttling Gold Nanoparticles into Tumoral Cells with an Amphipathic Proline-Rich Peptide. *ChemBioChem* **2009**, *10*, 1025–1031.
10. Ryan, J. A.; Overton, K. W.; Speight, M. E.; Oldenburg, C. N.; Loo, L.; Robarge, W.; Franzen, S.; Feldheim, D. L. Cellular Uptake of Gold Nanoparticles Passivated with BSA-SV40 Large T Antigen Conjugates. *Anal. Chem.* **2007**, *79*, 9150–9159.
11. Liu, Y.; Shipton, M. K.; Ryan, J.; Kaufman, E. D.; Franzen, S.; Feldheim, D. L. Synthesis, Stability, and Cellular Internalization of Gold Nanoparticles Containing Mixed Peptide-Poly(ethylene glycol) Monolayers. *Anal. Chem.* **2007**, *79*, 2221–2229.
12. Sun, L.; Liu, D.; Wang, Z. Functional Gold Nanoparticle-Peptide Complexes as Cell-Targeting Agents. *Langmuir* **2008**, *24*, 10293–10297.
13. Patel, P. C.; Giljohann, D. A.; Seferos, D. S.; Mirkin, C. A. Peptide Antisense Nanoparticles. *Proc. Natl. Acad. Sci. U.S.A.* **2008**, *105*, 17222–17226.
14. Oyelere, A. K.; Chen, P. C.; Huang, X.; El-Sayed, I. H.; El-Sayed, M. A. Peptide-Conjugated Gold Nanorods for Nuclear Targeting. *Bioconjugate Chem.* **2007**, *18*, 1490–1497.
15. Tkachenko, A. G.; Xie, H.; Liu, Y.; Coleman, D.; Ryan, J.; Glomm, W. R.; Shipton, M. K.; Franzen, S.; Feldheim, D. L. Cellular Trajectories of Peptide-Modified Gold Particle Complexes: Comparison of Nuclear Localization Signals and Peptide Transduction Domains. *Bioconjugate Chem.* **2004**, *15*, 482–490.
16. Tkachenko, A. G.; Xie, H.; Coleman, D.; Glomm, W.; Ryan, J.; Anderson, M. F.; Franzen, S.; Feldheim, D. L. Multifunctional Gold Nanoparticle-Peptide Complexes for Nuclear Targeting. *J. Am. Chem. Soc.* **2003**, *125*, 4700–4701.
17. Olmedo, I.; Araya, E.; Sanz, F.; Medina, E.; Arbiol, J.; Toledo, P.; Alvarez-Lueje, A.; Giralt, E.; Kogan, M. J. How Changes in the Sequence of the Peptide CLPFFD-NH_2 Can Modify the Conjugation and Stability of Gold Nanoparticles and Their Affinity for β-Amyloid Fibrils. *Bioconjugate Chem.* **2008**, *19*, 1154–1163.
18. Levy, R.; Thanh, N. T. K.; Doty, R. C.; Hussain, I.; Nichols, R. J.; Schiffrin, D. J.; Brust, M.; Fernig, D. G. Rational and Combinatorial Design of Peptide Capping Ligands for Gold Nanoparticles. *J. Am. Chem. Soc.* **2004**, *126*, 10076–10084.
19. Xie, H.; Tkachenko, A. G.; Glomm, W. R.; Ryan, J. A.; Brennaman, M. K.; Papanikolas, J. M.; Franzen, S.; Feldheim, D. L. Critical Flocculation Concentrations, Binding Isotherms, and Ligand Exchange Properties of Peptide-Modified Gold Nanoparticles Studied by UV-Visible, Fluorescence, and Time-Correlated Single Photon Counting Spectroscopies. *Anal. Chem.* **2003**, *75*, 5797–5805.
20. Liu, Y.; Franzen, S. Factors Determining the Efficacy of Nuclear Delivery of Antisense Oligonucleotides by Gold Nanoparticles. *Bioconjugate Chem.* **2008**, *19*, 1009–1016.
21. Nativo, P.; Prior, I. A.; Brust, M. Uptake and Intracellular Fate of Surface-Modified Gold Nanoparticles. *ACS Nano* **2008**, *2*, 1639–1644.
22. Wang, Z.; Levy, R.; Fernig, D. G.; Brust, M. Kinase-Catalyzed Modification of Gold Nanoparticles: A New Approach to Colorimetric Kinase Activity Screening. *J. Am. Chem. Soc.* **2006**, *128*, 2214–2215.
23. Duchesne, L.; Gentili, D.; Comes-Franchini, M.; Fernig, D. G. Robust Ligand Shells for Biological Applications of Gold Nanoparticles. *Langmuir* **2008**, *24*, 13572–13580.
24. Pengo, P.; Baltzer, L.; Pasquato, L.; Scrimin, P. Substrate Modulation of the Activity of an Artificial Nanoesterase Made of Peptide-Functionalized Gold Nanoparticles. *Angew. Chem., Int. Ed.* **2007**, *46*, 400–404.
25. De la Fuente, J. M.; Berry, C. C. Tat Peptide as an Efficient Molecule To Translocate Gold Nanoparticles into the Cell Nucleus. *Bioconjugate Chem.* **2005**, *16*, 1176–1180.
26. Maus, L.; Spatz, J. P.; Fiammengo, R. Quantification and Reactivity of Functional Groups in the Ligand Shell of PEGylated Gold Nanoparticles via a Fluorescence-Based Assay. *Langmuir* **2009**, *25*, 7910–7917.
27. Hostetler, M. J.; Templeton, A. C.; Murray, R. W. Dynamics of Place-Exchange Reactions on Monolayer-Protected Gold Cluster Molecules. *Langmuir* **1999**, *15*, 3782–3789.
28. Mammen, M.; Choi, S.-K.; Whitesides, G. M. Polyvalent Interactions in Biological Systems: Implications for Design and Use of Multivalent Ligands and Inhibitors. *Angew. Chem., Int. Ed.* **1998**, *37*, 2754–2794.
29. Dreaden, E. C.; Mwakwari, S. C.; Sodji, Q. H.; Oyelere, A. K.;

El-Sayed, M. A. Tamoxifen-Poly(ethylene glycol)-Thiol Gold Nanoparticle Conjugates: Enhanced Potency and Selective Delivery for Breast Cancer Treatment. *Bioconjugate Chem.* **2009**, *20*, 2247–2253.
30. Chien, Y.-Y.; Jan, M.-D.; Adak, A. K.; Tzeng, H.-C.; Lin, Y.-P.; Chen, Y.-J.; Wang, K.-T.; Chen, C.-T.; Chen, C.-C.; Lin, C.-C. Globotriose-Functionalized Gold Nanoparticles as Multivalent Probes for Shiga-Like Toxin. *ChemBioChem* **2008**, *9*, 1100–1109.
31. Gibson, J. D.; Khanal, B. P.; Zubarev, E. R. Paclitaxel-Functionalized Gold Nanoparticles. *J. Am. Chem. Soc.* **2007**, *129*, 11653–11661.
32. Turkevich, J.; Stevenson, P. C.; Hillier, J. The Nucleation and Growth Processes in the Synthesis of Colloidal Gold. *Discuss. Faraday Soc.* **1951**, 55–75, No. 11.
33. Frens, G. Controlled Nucleation for the Regulation of the Particle Size in Monodisperse Gold Suspensions. *Nat. Phys. Sci.* **1973**, *241*, 20–2.
34. Ji, X.; Song, X.; Li, J.; Bai, Y.; Yang, W.; Peng, X. Size Control of Gold Nanocrystals in Citrate Reduction: The Third Role of Citrate. *J. Am. Chem. Soc.* **2007**, *129*, 13939–13948.
35. Brown, K. R.; Walter, D. G.; Natan, M. J. Seeding of Colloidal Au Nanoparticle Solutions. 2. Improved Control of Particle Size and Shape. *Chem. Mater.* **2000**, *12*, 306–313.
36. Jana, N. R.; Gearheart, L.; Murphy, C. J. Seeding Growth for Size Control of 5−40 nm Diameter Gold Nanoparticles. *Langmuir* **2001**, *17*, 6782–6786.
37. Rodriguez-Fernandez, J.; Perez-Juste, J.; Garcia de Abajo, F. J.; Liz-Marzan Luis, M. Seeded Growth of Submicron Au Colloids with Quadrupole Plasmon Resonance Modes. *Langmuir* **2006**, *22*, 7007–10.
38. Zhong, C.-J. ; Njoki, P. N. ; Luo, J. , Controlled Synthesis of Highly Monodispersed Gold Nanoparticles. U.S. Patent Application 20070125196, July 07, 2005.
39. Niu, J.; Zhu, T.; Liu, Z. One-Step Seed-Mediated Growth of 30−150 nm Quasispherical Gold Nanoparticles with 2-Mercaptosuccinic Acid as a New Reducing Agent. *Nanotechnology* **2007**, *18*, 325607/1–325607/7.
40. Cao, L.; Zhu, T.; Liu, Z. Formation Mechanism of Nonspherical Gold Nanoparticles During Seeding Growth: Roles of Anion Adsorption and Reduction Rate. *J. Colloid Interface Sci.* **2006**, *293*, 69–76.
41. Grabar, K. C.; Freeman, R. G.; Hommer, M. B.; Natan, M. J. Preparation and Characterization of Au Colloid Monolayers. *Anal. Chem.* **1995**, *67*, 735–43.
42. Jana, N. R.; Gearheart, L.; Murphy, C. J. Evidence for Seed-Mediated Nucleation in the Chemical Reduction of Gold Salts to Gold Nanoparticles. *Chem. Mater.* **2001**, *13*, 2313–2322.
43. Ackerson, C. J.; Jadzinsky, P. D.; Kornberg, R. D. Thiolate Ligands for Synthesis of Water-Soluble Gold Clusters. *J. Am. Chem. Soc.* **2005**, *127*, 6550–6551.
44. Agasti, S. S.; You, C.-C.; Arumugam, P.; Rotello, V. M. Structural Control of the Monolayer Stability of Water-Soluble Gold Nanoparticles. *J. Mater. Chem.* **2008**, *18*, 70–73.
45. Zhang, F.; Skoda, M. W. A.; Jacobs, R. M. J.; Zorn, S.; Martin, R. A.; Martin, C. M.; Clark, G. F.; Goerigk, G.; Schreiber, F. Gold Nanoparticles Decorated with Oligo(Ethylene Glycol) Thiols: Protein Resistance and Colloidal Stability. *J. Phys. Chem. A* **2007**, *111*, 12229–12237.
46. Hong, R.; Fischer, N. O.; Verma, A.; Goodman, C. M.; Emrick, T.; Rotello, V. M. Control of Protein Structure and Function through Surface Recognition by Tailored Nanoparticle Scaffolds. *J. Am. Chem. Soc.* **2004**, *126*, 739–743.
47. Kanaras, A. G.; Kamounah, F. S.; Schaumburg, K.; Kiely, C. J.; Brust, M. Thioalkylated Tetraethylene Glycol: a New Ligand for Water Soluble Monolayer Protected Gold Clusters. *Chem. Commun.* **2002**, 2294–2295.
48. Weisbecker, C. S.; Merritt, M. V.; Whitesides, G. M. Molecular Self-Assembly of Aliphatic Thiols on Gold Colloids. *Langmuir* **1996**, *12*, 3763–3772.
49. Qian, X.; Peng, X.-H.; Ansari, D. O.; Yin-Goen, Q.; Chen, G. Z.; Shin, D. M.; Yang, L.; Young, A. N.; Wang, M. D.; Nie, S. In Vivo Tumor Targeting and Spectroscopic Detection with Surface-Enhanced Raman Nanoparticle Tags. *Nat. Biotechnol.* **2008**, *26*, 83–90.
50. Kumar, S.; Aaron, J.; Sokolov, K. Directional Conjugation of Antibodies to Nanoparticles for Synthesis of Multiplexed Optical Contrast Agents with Both Delivery and Targeting Moieties. *Nat. Protoc.* **2008**, *3*, 314–320.
51. Kim, D.; Park, S.; Lee, J. H.; Jeong, Y. Y.; Jon, S. Antibiofouling Polymer-Coated Gold Nanoparticles as a Contrast Agent for in Vivo X-ray Computed Tomography Imaging. *J. Am. Chem. Soc.* **2007**, *129*, 7661–7665.
52. Zheng, M.; Li, Z.; Huang, X. Ethylene Glycol Monolayer Protected Nanoparticles: Synthesis, Characterization, and Interactions with Biological Molecules. *Langmuir* **2004**, *20*, 4226–35.
53. Wuelfing, W. P.; Gross, S. M.; Miles, D. T.; Murray, R. W. Nanometer Gold Clusters Protected by Surface-Bound Monolayers of Thiolated Poly(ethylene glycol) Polymer Electrolyte. *J. Am. Chem. Soc.* **1998**, *120*, 12696–12697.
54. McIntosh, J. M.; Olivera, B. M.; Cruz, L. J.; Gray, W. R. γ-Carboxyglutamate in a Neuroactive Toxin. *J. Biol. Chem.* **1984**, *259*, 14343–6.
55. Hong, R.; Fernandez, J. M.; Nakade, H.; Arvizo, R.; Emrick, T.; Rotello, V. M. In Situ Observation of Place Exchange Reactions of Gold Nanoparticles. Correlation of Monolayer Structure and Stability. *Chem. Commun.* **2006**, 2347–2349.
56. The number of coupled peptides per particle (N_{pept}) is generally slightly higher for peptide **6** compared to **5**. This conclusion can only be made for AuNPs passivated with alkyl-PEG600 thiols (no place-exchange), while for AuNPs passivated with PEG3000 thiols, the number of coupled peptides cannot be controlled.
57. Mony, L.; Kew, J. N.; Gunthorpe, M. J.; Paoletti, P. Allosteric Modulators of NR2B-Containing NMDA Receptors: Molecular Mechanisms and Therapeutic Potential. *Br. J. Pharmacol.* **2009**, *157*, 1301–1317.
58. Paoletti, P.; Neyton, J. NMDA Receptor Subunits: Function and Pharmacology. *Curr. Opin. Pharmacol.* **2007**, *7*, 39–47.
59. Albensi, B. C. The NMDA Receptor/Ion Channel Complex: A Drug Target for Modulating Synaptic Plasticity and Excitotoxicity. *Curr. Pharm. Des.* **2007**, *13*, 3185.
60. Furukawa, H.; Singh, S. K.; Mancusso, R.; Gouaux, E. Subunit Arrangement and Function in NMDA Receptors. *Nature* **2005**, *438*, 185–192.
61. Donevan, S. D.; McCabe, R. T. Conantokin G is an NR2B-Selective Competitive Antagonist of *N*-Methyl-D-aspartate Receptors. *Mol. Pharmacol.* **2000**, *58*, 614–623.
62. Sheng, Z.; Liang, Z.; Geiger, J. H.; Prorok, M.; Castellino, F. J. The Selectivity of Conantokin-G for Ion Channel Inhibition of NR2B Subunit-Containing NMDA Receptors is Regulated by Amino Acid residues in the S2 Region of NR2B. *Neuropharmacology* **2009**, *57*, 127–136.
63. Prorok, M.; Castellino, F. J. The Molecular Basis of Conantokin Antagonism of NMDA Receptor Function. *Curr. Drug Targets* **2007**, *8*, 633–642.
64. Han, T. S.; Teichert, R. W.; Olivera, B. M.; Bulaj, G. Conus Venoms—A Rich Source of Peptide-Based Therapeutics. *Curr. Pharm. Des.* **2008**, *14*, 2462–2479.
65. Klein, R. C.; Prorok, M.; Galdzicki, Z.; Castellino, F. J. The Amino Acid Residue at Sequence Position 5 in the Conantokin Peptides Partially Governs Subunit-Selective Antagonism of Recombinant *N*-Methyl-D-aspartate Receptors. *J. Biol. Chem.* **2001**, *276*, 26860–26867.
66. Klein, R. C.; Galdzicki, Z.; Castellino, F. J. Inhibition of NMDA-Induced Currents by Conantokin-G and Conantokin-T in Cultured Embryonic Murine Hippocampal Neurons. *Neuropharmacology* **1999**, *38*, 1819–1829.
67. Ragnarsson, L.; Yasuda, T.; Lewis, R. J.; Dodd, P. R.; Adams, D. J. NMDA Receptor Subunit-Dependent Modulation by Conantokin-G and Ala(7)-Conantokin-G. *J. Neurochem.* **2006**, *96*, 283–291.
68. Kendrick, S. J.; Lynch, D. R.; Pritchett, D. B. Characterization of Glutamate Binding Sites in Receptors Assembled from Transfected NMDA Receptor Subunits. *J. Neurochem.* **1996**, *67*, 608–616.
69. Bresink, I.; Benke, T. A.; Collett, V. J.; Seal, A. J.; Parsons,

C. G.; Henley, J. M.; Collingridge, G. L. Effects of Memantine on Recombinant Rat NMDA Receptors Expressed in HEK 293 Cells. *Br. J. Pharmacol.* **1996**, *119*, 195–204.
70. Monyer, H.; Sprengel, R.; Schoepfer, R.; Herb, A.; Higuchi, M.; Lomeli, H.; Burnashev, N.; Sakmann, B.; Seeburg, P. H. Heteromeric NMDA Receptors: Molecular and Functional Distinction of Subtypes. *Science* **1992**, *256*, 1217–21.
71. Alkilany, A.; Murphy, C. Toxicity and Cellular Uptake of Gold Nanoparticles: What We Have Learned so Far. *J. Nanopart. Res.* **2010**, *12*, 2313–2333.
72. Zhu, Z.-J.; Ghosh, P. S.; Miranda, O. R.; Vachet, R. W.; Rotello, V. M. Multiplexed Screening of Cellular Uptake of Gold Nanoparticles Using Laser Desorption/Ionization Mass Spectrometry. *J. Am. Chem. Soc.* **2008**, *130*, 14139–14143.
73. Cheng, Y.; Samia, A. C.; Li, J.; Kenney, M. E.; Resnick, A.; Burda, C. Delivery and Efficacy of a Cancer Drug as a Function of the Bond to the Gold Nanoparticle Surface. *Langmuir* **2009**, *26*, 2248–2255.
74. Kharazia, V. N.; Weinberg, R. J. Immunogold Localization of AMPA and NMDA Receptors in Somatic Sensory Cortex of Albino Rat. *J. Comp. Neurol.* **1999**, *412*, 292–302.
75. Takumi, Y.; Ramirez-Leon, V.; Laake, P.; Rinvik, E.; Ottersen, O. P. Different Modes of Expression of AMPA and NMDA Receptors in Hippocampal Synapses. *Nat. Neurosci.* **1999**, *2*, 618–624.
76. Hardingham, G. E. ; Bading, H. Synaptic *versus* Extrasynaptic NMDA Receptor Signalling: Implications for Neurodegenerative Disorders. *Nat. Rev. Neurosci.* **2010**, *11*, 682– 696.
77. Pale-Grosdemange, C.; Simon, E. S.; Prime, K. L.; Whitesides, G. M. Formation of Self-Assembled Monolayers by Chemisorption of Derivatives of Oligo(Ethylene Glycol) of Structure $HS(CH_2)_{11}(OCH_2CH_2)_mOH$ on Gold. *J. Am. Chem. Soc.* **1991**, *113*, 12–20.
78. Prime, K. L.; Whitesides, G. M. Adsorption of Proteins onto Surfaces Containing End-Attached Oligo(Ethylene Oxide): A Model System Using Self-Assembled Monolayers. *J. Am. Chem. Soc.* **1993**, *115*, 10714–10721.
79. Lee, J. K.; Kim, Y.-G.; Chi, Y. S.; Yun, W. S.; Choi, I. S. Grafting Nitrilotriacetic Groups onto Carboxylic Acid-Terminated Self-Assembled Monolayers on Gold Surfaces for Immobilization of Histidine-Tagged Proteins. *J. Phys. Chem. B* **2004**, *108*, 7665–7673.
80. Orner, B. P.; Derda, R.; Lewis, R. L.; Thomson, J. A.; Kiessling, L. L. Arrays for the Combinatorial Exploration of Cell Adhesion. *J. Am. Chem. Soc.* **2004**, *126*, 10808–10809.
81. Chirakul, P.; Perez-Luna, V. H.; Owen, H.; Lopez, G. P.; Hampton, P. D. Synthesis and Characterization of Amine-Terminated Self-Assembled Monolayers Containing Diethylene Glycol Linkages. *Langmuir* **2002**, *18*, 4324–4330.